



# Electric Field Close to Lightning Channel in the Presence of Current Reflections from the Ground

Jovan Cvetic, Milan Ignjatovic, Milica Tausanovic,  
Nikola Mijajlovic, Dragan Pavlovic  
School of Electrical Engineering  
Belgrade, Serbia  
cvetic\_j@etf.rs

Fridolin Heidler  
University of the Federal Armed Forces  
Faculty of Electrical Engineering, EIT 7  
Munich, Germany  
Fridolin.Heidler@unibw-muenchen.de

**Abstract**—Appearance of an overcompensated positive electric field in most vertical field measurements performed very close to the channel core is explained using the extended generalized traveling current source (extended GTCS) return stroke model with current reflections from the ground. New effects in the corona sheath due to the reflection of current pulses have been noted and taken into account. The channel-base current is separated into two components. The first current component is fast and with a greater peak value, while the second component is slower and with a lower peak. We've analyzed a return stroke for which the channel-base current and the electric field waveform very close to the triggered lightning are measured simultaneously. A new charging function is calculated according to the extended GTCS model, as well as the value of the ground reflection coefficient for the analyzed stroke. On one hand, new results are obtained through calculations of the channel charging function. On the other, the calculated values of the ground reflection coefficient confirm the results reported in other independent studies performed in natural or laboratory conditions. Finally, the concept of the extended GTCS model, that takes into account current pulse reflections from the ground, is proved to be correct.

**Keywords** - *Lightning electromagnetic pulse, ground reflections, corona sheath dynamics, return stroke model*

## I. INTRODUCTION

Lightning channel charge and its distribution along the channel prior to a return stroke plays a crucial role in the generation of the current at the channel base. As a result, these determine the electric and magnetic fields near the channel, which are usually measured. By means of appropriate corona sheath and return stroke models, these field waveforms are used for examining the dynamics of the corona envelope during discharge.

Dart leader channel charge has been determined in [1] to be a minimum of 0.2 C, with the most frequent value between 0.5 and 1 C. These values also agree with the charge brought to ground by subsequent strokes, [2].

A rough estimation of the way in which dart leader charge is distributed along the channel can be obtained through a numerical procedure, using charge simulation methods, by treating the dart leader as a conducting channel connected to a spherical electrode with a radius of several kilometers, raised

to the potential of a cloud, [3]. Baum's model [4] of the dart leader charge distribution prior to the return stroke assumed that the corona envelope is in the shape of an inverted circular cone, a few tens of meters in size, at the bottom of the leader channel. Charge density in Baum's model is zero at the ground and increases linearly with height.

The existence of two zones around the lightning channel core during the return stroke stage is inferred in [5, 6], Fig.2. The inner zone (zone 1) surrounds the channel core and contains net positive charge, while the outer zone (zone 2), which surrounds zone 1, contains negative charge, with net charge inside the entire corona sheath being zero after the return stroke stage.

Two improved models for predicting charge motion in the corona sheath were proposed in [6]. The new results and details of measurements from [7] were published later [8]. They have provided new insights and the explanation of the corona discharge during the return stroke. They also demonstrated the existence of a positive overcompensated electric field in over two thirds of measured field waveforms. These measurements indicate that complete dissipation of the corona sheath charge (or the corresponding electric field) takes place within milliseconds, long after the channel-base current has ceased to flow.

The new corona sheath model developed in this study represents an improved model of the corona sheath described in earlier studies [5], [6], [9]. Corona models in these studies were also in accordance with the experiments of corona discharges in coaxial geometry [10]. The new extended GTCS model with current reflections from the ground [11] has been applied to make these improvements possible. Effects observed in measurements [7], [8], regarding the existence of a positive overcompensated electric field, are explained herein. Furthermore, effects regarding transient ground impedances, observed in both triggered lightning conditions [12] and in return strokes simulated in the laboratory [13], [14], are also confirmed in our present study.

## II. CHANNEL-BASE CURRENT

Calculations of the channel charging function in the extended GTCS, which are needed for the calculations of

corona sheath dynamics, involve the channel-base current. One analytical current waveform which is very convenient for fitting involves the Heidler's function [15]. The best fit of the measured current curve is obtained when the existence of two channel-base current components is taken into account. Total channel-base current can be expressed as

$$i_0(t) = \sum_{i=1}^2 I_{mi} \left\{ (t/\tau_{ci})^{n_{ci}} / [1 + (t/\tau_{ci})^{n_{ci}}] \right\} \exp(-t/\tau_{c2i}), \quad (1)$$

where  $I_{mi}$  is the current amplitude,  $\tau_{ci}$  and  $\tau_{c2i}$  are the first and the second discharge time constants (determining the leading and the trailing edge of the current pulse, respectively), and  $n_{ci}$  is the current steepness factor (where index  $i$  denotes the corresponding current component). For our analysis, we have adopted the channel-base current pulse from stroke 1 in flash S0033, along with the corresponding electric field waveform [7, 8]. Values of channel-base current parameters in (1) are presented in Table I. The measured curve and the fitted current components are shown in Fig. 1, [16].

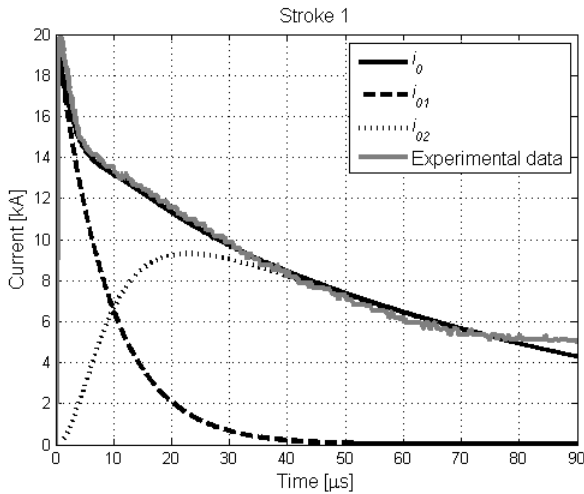


Figure 1. Measured channel-base current waveform for stroke 1 in flash S0033, [7, 8] and its curve fit separated into two components [16].

### III. A NEW CORONA SHEATH MODEL

Given that the measurements [8] indicate that complete dissipation of the corona sheath charge (or the corresponding electric field) takes place within milliseconds, long after the channel-base current has ceased to flow, our interpretation was that negative leader charge is overcompensated by the positive charge in the channel sheath. In other words, there is a certain excess of positive charge generated during the return stroke which remains in the corona sheath after the channel-base current has ceased to flow. This conclusion was a consequence of an earlier analysis which had showed that the maximum

extent of the leader sheath radius was 6 cm ([9], Table IV therein). Since the electric field sensor was positioned at 10 cm from the channel core, our assumption is that the measurements were performed outside the maximum perimeter of the corona envelope (denoted by  $R_2$  and calculated below). The obtained results support this view, but don't dismiss the applicability of other corona sheath models with different initial assumptions. Although at first glance it may seem strange that the corona sheath is charged with overcompensated positive charge, detailed analysis shows that this is a more or less straightforward result, which emerges as a consequence of an incomplete current pulse reflection from the ground. This effect couldn't have been noted earlier, using other traveling-current-source (TCS) models without current reflections, such as the original TCS model described in [15], or any of later TCS models [17-19]. As stated above, the recently proposed extended GTCS model [11] with current reflections from the ground enabled the observed effect to be calculated.

TABLE I. THE VALUES OF THE PARAMETERS IN (1), [16]

Fit curve	$I_{mi}$ [kA]	$n_{ci}$	$\tau_{ci}$ [ $\mu$ s]	$\tau_{c2i}$ [ $\mu$ s]
$i_{01}, i=1$	20.403	4	71.801	8.7766
$i_{02}, i=2$	15.228	2	9.9791	0.19364

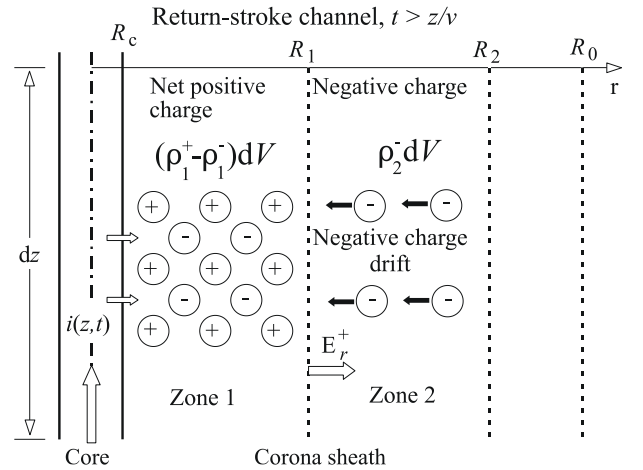


Figure 2. Leader channel during the return stroke stage, composed of a narrow core with radius  $R_c$  and a negative charged corona sheath (itself consisting of two zones). Negative charges drift from zone 2 to zone 1, so that charge in zone 2 decays exponentially, while  $R_2$  remains constant. Positive and negative space charges in zone 1 are  $\rho_1^+$  and  $\rho_1^-$ , respectively,  $\rho_2^-$  is the negative space charge in zone 2.  $E_r^+$  and  $E_r^-$  are the breakdown field at the outer boundary of zones 1 and 2, respectively. Adopted from [6].

#### IV. THE EXTENDED GTCS MODEL

In the extended GTCS model [11] the downward moving current pulse  $i_{0,d}$  is reflected from the ground generating the upward moving current pulse

$$i_{0,u} = \Gamma i_{0,d} \quad (2)$$

where  $|\Gamma| \leq 1$  is the ground reflection coefficient and

$$i_{0,d}(t) = \int_0^{h_a} q_0^+ \frac{\partial}{\partial t} f^+(t - z/v^*) dz, \quad t > z/v^*, \quad (3)$$

where  $f^+(u)$  is the channel charging function,  $h_a = v^*t$  is the apparent channel height,  $v^* = vc/(v+c)$ ,  $v$  is the return stroke speed,  $z$  is the channel altitude and  $q_0^+$  is the positive input line charge that completely neutralizes initial leader line charge density. Theoretically, if the conductivity of the ground is infinite, the value of the ground reflection coefficient equals 1. But for well-grounded structures (e.g. towers) with finite ground conductivity, it has a value below 1. For instance, the Peissenberg tower (Germany) has the ground reflection coefficient of about  $\Gamma = 0.7$ , [20].

In case  $\Gamma = 0$ , ground reflections are ignored, as it is a priori assumed in [15], [17-19]. However, its value has a strong nonlinear dependence on the magnitude of the channel-base current, [12-14]. This issue is discussed in the next section and included in the extended GTCS model.

The sum of the downward and the upward current components produces the total current at the channel base

$$i_0(t) = i_{0,d}(t) + i_{0,u}(t) = (1 + \Gamma)i_{0,d}(t). \quad (4)$$

Current pulses travel along the perfectly conducting channel core at the speed of light, without attenuation. According to theoretical results derived in [21] for TCS-type models, the transition line charge densities along the channel core due to downward and upward propagating current pulses in the core are  $-i_{0,d}(t)/c$  and  $i_{0,u}(t)/c$ , respectively. Using (2) and (4), total transition line charge near the channel bottom can be expressed as

$$q_{tr}(t) = (i_{0,u} - i_{0,d})/c = -(1 - \Gamma)/(1 + \Gamma)i_0(t)/c. \quad (5)$$

In usual conditions  $0 \leq \Gamma < 1$  and the total transition line charge given by (5) is negative. In order to take its nonlinear behavior into account, we introduced a time-dependent function for  $\Gamma$ , with two sets of parameters corresponding to the two channel-base current components given by (1).

#### V. GROUND REFLECTION COEFFICIENT

When lightning is applied to a grounding device, the current disperses into the earth through the device. When the electric field in soil, close to the grounding device, exceeds a critical breakdown field, the soil breaks [22], [23], [14].

An extended research of the most suitable time-dependent function for the ground reflection coefficient settled on the function with an exponential form

$$\Gamma_i(t) = \Gamma_{0i} \exp(-k_i t), \quad i = 1, 2 \quad (6)$$

where  $\Gamma_{0i}(i_{0i})$  is the nonlinear ground reflection coefficient at the striking point (dependant on the peak current) and  $k_i$  is the exponential decay constant. Behavior of reflection coefficients takes into account the change of ground resistance during the return stroke in the following way:

(a) For the fast current component  $i_{01}$ , Fig.1 and Table II, with a peak value exceeding 15 kA, sparking zone is formed in the soil, which causes ground resistance to drop to a very low value, which then subsists until the end of the return stroke. In our approximation, soil resistivity is zero, which creates a great mismatch between impedances of the channel and the ground. Current pulses are fully reflected, i.e. the ground reflection coefficient is  $\Gamma_1 = 1$ . Since the rise time of the first current component in stroke 1 ( $i_{01}$ ) is very short (below 1  $\mu$ s, Fig.1), this value is attained at the very beginning of discharge ( $t \approx 0$  in (6)). According to (5) there is no transition line charge due to the reflection of this current component.

(b) For the slower current component  $i_{02}$ , with a lower peak value (below 15 kA), the ground reflection coefficient  $\Gamma_{02}$  is less than 1. According to (5), the reflection of this current component always generates additional (negative) transition line charge along the core.

TABLE II. GROUND REFLECTION COEFFICIENTS (6), [3]

Flash S0033			Ground reflection coefficient	
Stroke 1	$i_{01}$	>15kA	$\Gamma_{01} = 1$	$k_1 = 0$
	$i_{02}$	<15kA	$\Gamma_{02} = 0.9$	$k_2 = 2600\text{s}^{-1}$

#### VI. ELECTRIC FIELD IN THE CORONA SHEATH

The model of the charge neutralization process during the return stroke used in the present study is based on theoretical and experimental studies of corona discharges in coaxial geometry performed in laboratory. Theoretical considerations about the similarities of these lab results to those from real lightning discharges are to be found in [24].

Expression for the radial electric field close to the negatively charged channel corona sheath during a return stroke is adopted from [9]

$$E = q_0^+ / (2\pi\epsilon_0 r) [f^+(u) - 1], \quad (7)$$

where  $q_0^+$  is the absolute value of initial (leader) line charge density at the height where measurements are conducted.

Equation (7) is derived without taking into account the transition line charge density along the channel core, which can be neglected near the striking point assuming ground is perfectly conducting. In that case, the value of the ground reflection coefficient equals 1, [9].

According to (5), an additional field term caused by negative transition line charge density along the core should be added to (7), which yields

$$E = \frac{q_0^+}{2\pi\epsilon_0 r} (f^+ - 1) + \frac{q_{tr}}{2\pi\epsilon_0 r}, \quad (8)$$

where  $r=0.1$  m [7, 8] and

$$q_{tr} = -\frac{1}{c} \sum_{i=1}^2 i_{0i}(t) \frac{1-\Gamma_i(t)}{1+\Gamma_i(t)}. \quad (9)$$

Rearranging the terms in (8) leads to

$$f^+(t) = 1 + \frac{2\pi\epsilon_0 r E}{q_0^+} + \frac{1}{q_0^+ c} \sum_{i=1}^2 i_{0i}(t) \frac{1-\Gamma_i(t)}{1+\Gamma_i(t)}. \quad (10)$$

Since within the extended GTCS all functions are causal (e.g.  $f^+(0) = 0$ , because  $i_{01}(0) = 0$  and  $i_{02}(0) = 0$ ), it follows that

$$q_0^+ = -2\pi\epsilon_0 r E(0) \quad (11)$$

It is clear from (10) that after a certain time, which depends on the values of other parameters in (10), the channel charging function has a positive overshoot ( $f^+ > 1$ ) if  $\Gamma_1 < 1$  and/or  $\Gamma_2 < 1$ . For example, it occurs at about 10  $\mu\text{s}$  for stroke 1 in flash S0033, [7, 8], Fig.3. In other words, due to the presence of the negative transition line charge during the return stroke phase, more positive charge is pumped into the corona sheath. The positive charge overcompensates the negative charge delivered previously by the leader. This issue is elaborated upon in the next section. Expression used for curve fits of the measured electric field is

$$E(t) = \sum_{i=1}^2 E_{mi} \left\{ (t/\tau_{E1i})^{n_{Ei}} / [1 + (t/\tau_{E1i})^{n_{Ei}}] \right\} \exp(-t/\tau_{E2i}), \quad (12)$$

where  $E_{mi}$  is the electric field magnitude,  $\tau_{E1i}$  and  $\tau_{E2i}$  are the first and second discharge time constants determining the leading and the trailing edge of the electric field pulse, respectively, and  $n_{Ei}$  is the electric field steepness factor (where index  $i$  denotes the corresponding electric field component). For best matching with measured field waveforms, the fitted curves are separated into two components, with the parameters given in Table III. In further analysis, we used the corona model with charge diffusion in the corona sheath, that is with an exponential decay of negative charge in zone 2, as suggested in [6]. Negative charge penetrates zone 1 from zone 2, with a decay time constant  $\tau_d$  that reflects the reduction of negative charge deposited within zone 2 (Fig. 2). It should be noted that

negative charge drifting from zone 2 into zone 1 can be viewed as positive charge drifting in the opposite direction.

TABLE III. VALUES OF THE PARAMETERS IN (12), [16]

Flash S0033	Fit curve	$E_{mi}$ [MV/m]	$n_{Ei}$	$\tau_{E1i}$ [ $\mu\text{s}$ ]	$\tau_{E2i}$ [ $\mu\text{s}$ ]
Stroke 1	$E_1, i=1$	-2.336	0	1	50
	$E_2, i=2$	1.244	1.1357	1.0982	59.215

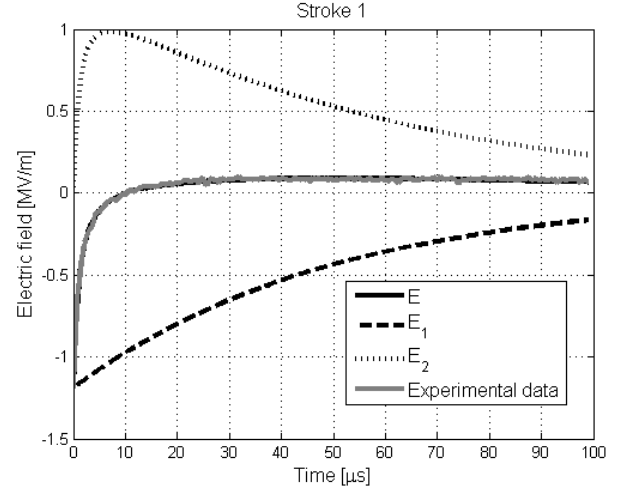


Figure 3. Measured and fitted curves of the electric field waveforms for stroke 1 in flash S0033, [7, 8] separated into two components according to (12). Values of parameters are given in Table III, [16].

Maximum extent of the corona is defined by the initial leader line charge density  $q_0^+$  (11) and by the absolute value of the critical breakdown electric field at the outer corona sheath boundary  $|E_r^-|$ , Table IV

$$R_2 = q_0^+ / (2\pi\epsilon_0 |E_r^-|) = Const. \quad (13)$$

TABLE IV. INITIAL CHANNEL SHEATH PARAMETERS, [16]

Flash S0033 [7, 8]	Peak electric field [MV/m]	$q_0^+$ [ $\mu\text{C}/\text{m}$ ] (11)	Initial channel sheath radius $R_2$ [cm] (13)	Breakdown electric field at $R_2$ , $ E_r^- $ [MV/m] [4]
Stroke 1	1.168	6.67	6	2

Applying Gauss' law to an elementary cylinder with top and bottom faces with radius  $R_1$  one obtains

$$2\pi\epsilon_0 E_r^+ R_1 = -q_0^+ + \rho_0^- e^{-t/\tau_d} [R_2^2 - R_1^2] + q_0^+ f^+ + q_{tr}, \quad (14)$$

where  $\rho_0^- \cong -(2\pi\epsilon_0 |E_r^-|)^2 / (\pi q_0^+)$ . Variables  $q_{tr}$ ,  $R_2$  and  $f^+$  are given by (9), (13) and (16), respectively. Radius  $R_1$  of zone 1 is obtained by solving (14) simultaneously with (16).

## VII. THE CHANNEL CHARGING FUNCTION

Discharge of the channel core is caused by the potential difference  $U_{C0}$  between the core ( $R_C$ ) and the distant reference point ( $R_0$ ) on the ground, as shown in Fig.2. If the core and the ground are treated as perfect conductors, the potential difference is zero, that is  $U_{C0} = 0$ . Despite this simplification, we have achieved very good agreement of the theory with experimental data. The voltage drop  $U_{C0}$  can be expressed as

$$U_{C0} = \int_{R_c}^{R_1} E_{in} dr + \int_{R_1}^{R_0} E_{out} dr + \int_{R_c}^{R_2} E_{R1} dr + \int_{R_2}^{R_0} E_{out} dr + \int_{R_c}^{R_0} E_{tr} dr. \quad (15)$$

where  $R_0$  is the radial distance from the channel core to the reference point on the ground,  $E_{inR1}$ ,  $E_{outR1}$ ,  $E_{R1R2}$ ,  $E_{outR2}$  and  $E_{tr}$  are the electric fields inside  $R_1$ , outside  $R_1$  (due to charge inside  $R_1$ ), between  $R_1$  and  $R_2$  (due to the charge closed between  $R_1$  and  $R_2$ ), outside  $R_2$  (due to total charge between  $R_1$  and  $R_2$ ) and the transition field due to transition charge, respectively, [16]. Equation (15) leads to

$$f^+ = f_0^+ + f_{ad}^+, \quad (16)$$

where

$$f_0^+ = \left\{ \frac{1}{2q_0^+} \left\{ q_0^+ + k\rho_0^- \pi e^{-t/\tau_d} \right\} + \left\{ 1 + \frac{k\rho_0^- \pi e^{-t/\tau_d}}{q_0^+} \right\} \ln \frac{R_0}{R_1} \right\} / \left[ 0.5 + \ln \left( \frac{R_0}{R_1} \right) \right], \quad k = R_2^2 - R_1^2, \quad (17)$$

is the channel charging function without the influence of the transition charge and

$$f_{ad}^+(t) = \frac{\ln(R_0/R_c)}{cq_0^+} \left[ \sum_{i=1}^2 i_{0i}(t) \frac{1-\Gamma_i}{1+\Gamma_i} \right] / \left[ \frac{1}{2} + \ln \left( \frac{R_0}{R_1} \right) \right], \quad (18)$$

represents the additional channel charging function due to the influence of the transition charge. Variables  $R_1$  and  $\tau_d$  are the radius of zone 1 [16] and the charge decay constant in zone 2, respectively [6].

## VIII. RESULTS OF THE CALCULATIONS AND DISCUSSION

The channel charging function and its components calculated by (16), (17) and (18) are shown in Fig.4. In Fig.5 measured (12) and calculated (8) curves of the electric field are depicted. The graphs show overall good matching, with discrepancies noticed only at the beginning of the discharge, due to the complex nature of ground reflection. Equation (6) with the parameters given in Table II is too simple to describe the nonlinear behavior of ground reflection during the return stroke in its entirety. But in this stage of the investigation we adopted (6) as a first rough approximation.

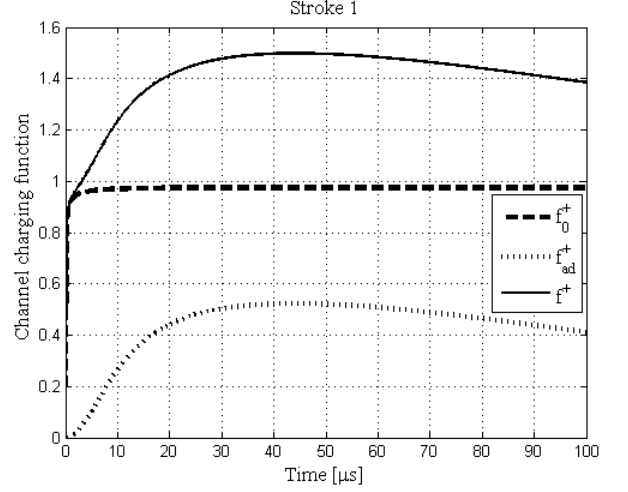


Figure 4. The channel charging function vs time during return stroke 1 in flash S0033, [7], [8]. The channel-base current and the electric field curve fits are given by (1) and (12), respectively, with the parameters given in Tables I and III. Solid line represents the total channel charging function  $f^+ = f_0^+ + f_{ad}^+$ . Values of other parameters for the calculations are  $E_r^+ = 1 \text{ MV/m}$ ,  $|E_r^-| = 2 \text{ MV/m}$ ,  $\tau_d = 650 \mu\text{s}$ , channel core radius is  $R_c = 0.5 \text{ cm}$ . The distance of the reference point is  $R_0 = 100 \text{ m}$ .

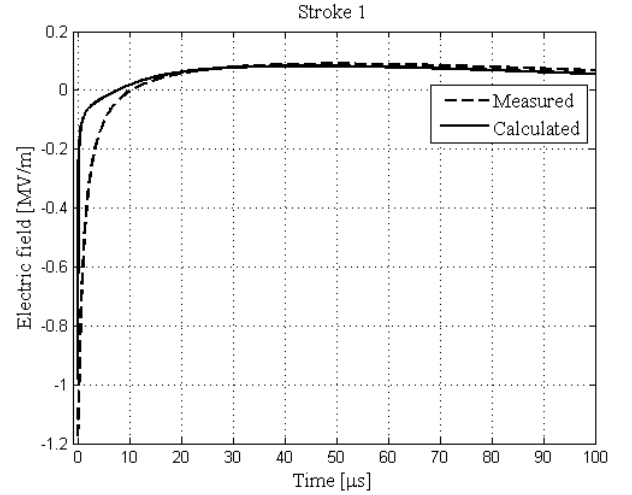


Figure 5. Measured (12) and calculated (8), (16) curves of the electric field vs time during return strokes 1 in flash S0033, [7], [8]. Values of all other parameters are the same as in Fig.4.

According to (4), for a particular  $i$ -th channel-base current component, the corresponding downward moving current is  $i_{0i}/(1+\Gamma_i)$ . Applying (4) again to the total channel-base current, one can define the total ground reflection coefficient during the return stroke as

$$\Gamma_{tot} = i_0 / \sum_{i=1}^2 i_{0i} / (1+\Gamma_i) - 1. \quad (19)$$

Total ground reflection coefficient versus channel-base current is presented in Fig.6.

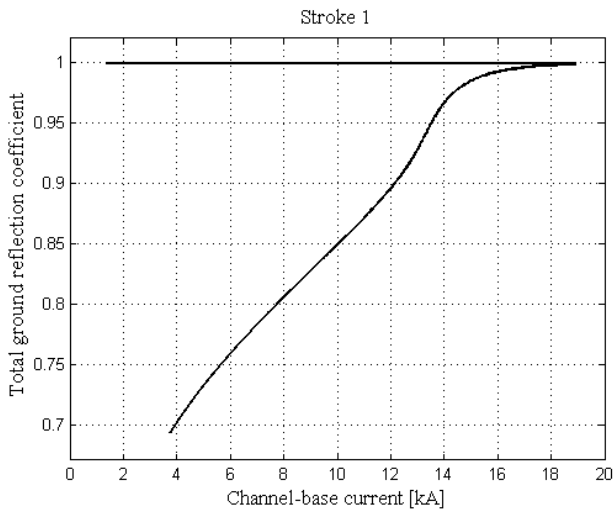


Figure 6. Total ground reflection coefficient versus channel-base current according to (19) during the return strokes 1 in flash S0033, [7, 8] with the parameters given in Tables I, II and III. Values of all other parameters are the same as in Fig.4.

A strong nonlinear behavior with a hysteresis can be noticed. It is obvious that the total ground reflection coefficient attains the value of 1 (due to the formation of a sparking zone with very low resistivity in the soil for the current peak above 15 kA, [14]) at the very beginning of the discharge. As a result, this coefficient retains a relatively high value during the discharge. This in turn decreases the transition charge (9) and the corresponding charging function (18). Consequently, less positive (overcompensated) charge is pumped into the corona sheath in zone 1, generating a lower positive electric field, Fig.5.

## IX. CONCLUSION

We've analyzed a return stroke for which the channel-base current and the electric field waveform very close to the triggered lightning are measured simultaneously. A new charging function according to the extended GTCS model is calculated, as well as the value of the ground reflection coefficient for the analyzed stroke. New results of channel charging function calculations are presented in the paper. Moreover, the ground reflection coefficient is calculated confirming the results reported in other independent studies performed in natural or laboratory conditions. Finally, the concept of the extended GTCS model that takes into account current pulse reflections from the ground is proved to be correct.

## ACKNOWLEDGMENT

Ministry of Science and Technological Development of the Republic of Serbia supported this work under contracts No. 171007 and 37019.

## REFERENCES

[1] M. Brook, N. Kitagawa, E. J. Workman, Quantitative study of strokes and continuing currents in lightning discharges to ground, *J. Geophys. Res.*, 67 (1962), pp.649–659.

[2] K. Berger, Methoden und Resultate der Blitzforschung auf dem Monte San Salvador bei Lugano in den Jahren 1963–1971, *Bull. Schweiz. Elektrotech. Ver.*, 63 (1972), pp.1403–1422.

[3] A. Larsson, V. Cooray, Charge distribution in the lightning leader channel, *Proceedings of 23rd international conference on Lightning protection, Italy, 1996*, pp.56–60.

[4] C. E. Baum, Return stroke initiation, In *Lightning Electromagnetics*, ed. R.L. Gardner, New York: Hemisphere (1990), pp. 101–14.

[5] G. Maslowski, V.A. Rakov, A study of the lightning channel corona sheath, *J. Geophys. Res.*, 111(D14110) (2006) doi:10.1029/2005JD006858.

[6] G. Maslowski, V. A. Rakov, J. M. Cvetic, M. Miki, An Improved Model for Prediction of the Dynamics of Lightning Channel Corona Sheath, *20th Int. Zurich Symposium on EMC, Zurich, 2009*.

[7] M. Miki, V.A. Rakov, K. J. Rambo, G.H. Schnetzer, M.A. Uman, Electric field near triggered lightning channels measured with Pockels sensors, *J. Geophys. Res.*, 107 (D16) (2002) ACL 2-1–ACL 2-11.

[8] G. Maslowski, V.A. Rakov, M. Miki, Some Inferences From Radial Electric Fields Measured Inside the Lightning-Channel Corona Sheath, *IEEE Trans. on Electromagnetic Compatibility*, 53 (2) (2011) 390-394.

[9] J. Cvetic, F. Heidler, S. Markovic, R. Radosavljevic, P. Osmokrovic, Dynamics of a lightning corona sheath—A constant field approach using the generalized traveling current source return stroke model, *Journal of Atmospheric Research* 117 (2012) 122–131.

[10] V. Cooray, Charge and Voltage Characteristics of Corona Discharges in a Coaxial Geometry, *IEEE Transaction on Dielectrics and Electrical Insulation*, 7(6) (2000) 734-743.

[11] M. Ignjatovic, J. Cvetic, D. Pavlovic, R. Djuric, M. Ponjavic, D. Sumarac, Z. Trifkovic, N. Mijajlovic, Generalized Traveling Current Return Stroke Model with Current Reflections and Attenuation Along the channel, *32<sup>nd</sup> ICLP, Shanghai, China, 2014*, p.32-36.

[12] V.A Rakov, M.A Uman, K.J. Rambo et al., New insights into lightning processes gained from triggered-lightning experiments in Florida and Alabama, *J. Geophys. Res.*, 103 (D12) (1998), 14.117–14.130.

[13] R. Kosztaluk, M. Loboda, D. Mukhedkar, Experimental study of transient ground impedances, *IEEE Transactions on Power Apparatus and Systems*, Vol. PAS-100,11 (1981), 4653-4660.

[14] J.P. Wang, A.C. Liew, M. Darveniza, Extension of dynamic model of impulse behavior of concentrated grounds at high currents, *IEEE Transactions on Power Delivery*, 20 (3) (2005), 2160–2165.

[15] F. Heidler, TCS model for LEMP calculation, *6th Symposium on EMC, Zurich, (1985)* 157-162.

[16] M.Tausanovic, M.Ignjatovic, J.Cvetic, F. Heidler, M. Alimpijevic, D. Pavlovic “Influence of Current Reflections from the Ground on Corona Sheath Dynamics during the Return Stroke,” unpublished.

[17] G. Diendorfer, M. Uman, An Improved Return Stroke Model with Specified Channel-base Current, *J. Geop. Res.*, 95 (1990) 13621-13644.

[18] R. Thottappillil, M.A. Uman, Lightning return stroke model with height-variable discharge time constant, *J. Geop. Res.*, 99 (1994) 22773-22780.

[19] J. Cvetic, B.Stanic, An Improved Return Stroke Model with Specified Channel-base Current and Charge Distribution along Lightning Channel, *International Conference on Electromagnetics in Advanced Application (ICEAA), Torino, Italy, 1995*.

[20] F. Fuchs, On the transient behavior of the telecommunication tower at the mountain Hoher Peissenberg, in *Proc. 27th ICLP, Birmingham, UK, 1998*, pp. 36-41.

[21] R. Thottappillil, V. Rakov, M. Uman, Distribution of charge along the lightning channel: Relation to remote electric and magnetic fields and to return stroke models, *J. of Geophys. Res.*, 102 (D6) (1997) 6987-7006.

[22] H.M. Towne, Impulse characteristics of driven grounds, *General Electric Review* (1929), 605–609.

[23] S. Sekioka, M.I. Lorentzou, M.P. Philippakou, J.M. Prousalidis, Current-dependent grounding resistance model based on energy balance of soil ionization, *IEEE Trans. on Power Delivery*, 21 (1) (2006), 194–201.

[24] J. Cvetic, F. Heidler, S. Markovic, R. Radosavljevic, P. Osmokrovic, Dynamics of a lightning corona sheath—A constant field approach using the generalized traveling current source return stroke model, *Journal of Atmospheric Research* 117 (2012) 122–131.